

Orbital-corrected orbital-free density functional theory

Baojing Zhou and Yan Alexander Wang^{a)}

Department of Chemistry, University of British Columbia, Vancouver, British Columbia V6T 1Z1, Canada

(Received 14 November 2005; accepted 23 January 2006; published online 28 February 2006)

A new implementation of density functional theory (DFT), namely orbital-corrected orbital-free (OO) DFT, has been developed. With at most two non-self-consistent iterations, OO-DFT accomplishes the accuracy comparable to fully self-consistent Kohn-Sham DFT as demonstrated by its application on the cubic-diamond Si and the face-centered-cubic Ag systems. Our work provides a new impetus to further improve orbital-free DFT method and presents a robust means to significantly lower the cost associated with general applications of linear-scaling Kohn-Sham DFT methods on large systems of thousands of atoms within different chemical bonding environment.

© 2006 American Institute of Physics. [DOI: 10.1063/1.2176610]

Density functional theory (DFT) has been firmly established as one of the most widely used first-principles quantum mechanical (QM) methods in many fields.^{1–5} Each of the two ways of solving the DFT problem, i.e., the traditional orbital-based Kohn-Sham (KS)^{3,4} and the orbital-free (OF)⁵ schemes, has its own strengths and weaknesses. In this Communication, we present a new implementation of DFT, namely orbital-corrected orbital-free (OO) DFT, which coalesces the advantages and avoids the drawbacks of OF-DFT and KS-DFT and allows systems within different chemical bonding environment to be studied at a much lower cost than the traditional self-consistent KS-DFT method. Furthermore, OO-DFT can achieve linear scaling by employing currently available linear-scaling KS-DFT algorithms and provide a powerful tool to treat large systems of thousands of atoms much more efficiently than other currently available linear-scaling DFT methods.

In the traditional KS-DFT,³ the computational cost scales like $\mathcal{O}(N_k \cdot N^3)$, where N is a measure of the system size (the size of the basis set or the number of electrons) and N_k is the number of the \mathbf{k} -points used in the Brillouin-zone sampling required for periodic systems.⁶ In the last decade, many linear-scaling techniques have been developed to reduce the scaling of KS-DFT.⁴ With such techniques, one could solve the KS equations under a fixed effective potential with a cost increasing linearly with the system size.³⁸ The efficiency of these linear-scaling techniques is further enhanced by combining them with massively parallel algorithms.⁷ Recently, systems of more than 1000 atoms have been studied with such state-of-the-art linear-scaling techniques.^{7,8} Despite their success, these methods still suffer from a severe disadvantage, which is the number of many iterations required to achieve self-consistency,^{9,10} whose computational cost per iteration is still quite high.

On the other hand, if a good approximation of the exact density or the exact wave function is already known, one can avoid the many iterations in the self-consistent KS-DFT by using efficient perturbation techniques to calculate the den-

sity or the wave function. A good example is the famous Harris functional^{11,12} with incomplete inclusion of the second-order correction. Based on the same perturbation approach, a new method incorporating the complete second-order correction was recently developed by Benoit *et al.*¹³ and further modified by Zhu and Trickey.¹⁴ One difficulty of this method is the necessity to evaluate the second-order functional derivative of the exchange-correlation energy density functional (XCEDF). It also remains to be investigated under what circumstances this method is suitable for applications on large systems, with a comparable accuracy to the fully self-consistent KS-DFT.

From a different perspective, the original Hohenberg-Kohn (HK) theorems of DFT² involve no orbitals at all and the total energy is formulated purely as a functional of the electron density $\rho(\mathbf{r})$ for a given external potential $v_{\text{ne}}(\mathbf{r})$,

$$E_v[\rho] = T_s[\rho] + E_H[\rho] + E_{\text{xc}}[\rho] + \langle \rho(\mathbf{r})v_{\text{ne}}(\mathbf{r}) \rangle, \quad (1)$$

where T_s is the electronic kinetic energy of a noninteracting system that has the same electron density as the interacting system, E_H is the classical Hartree repulsion energy, E_{xc} is the exchange-correlation energy, and $\langle \rho(\mathbf{r})v_{\text{ne}}(\mathbf{r}) \rangle$ is a shorthand notation for the nuclear-electron interaction energy, $\int \rho(\mathbf{r})v_{\text{ne}}(\mathbf{r})d\mathbf{r}$. In fact, the original implementation of DFT, namely the Thomas-Fermi (TF) model,¹⁵ is an OF scheme, in which $\rho(\mathbf{r})$ is the only variational variable. In OF-DFT, one can calculate the ground-state density and other properties not explicitly dependent on the wave function, by directly minimizing Eq. (1) under the constraint that $\rho(\mathbf{r})$ is properly normalized to the number of electrons in the system. This leads to the following TF-HK equation,

$$\begin{aligned} \frac{\delta E_v[\rho]}{\delta \rho(\mathbf{r})} &= \frac{\delta T_s[\rho]}{\delta \rho(\mathbf{r})} + \frac{\delta E_H[\rho]}{\delta \rho(\mathbf{r})} + \frac{\delta E_{\text{xc}}[\rho]}{\delta \rho(\mathbf{r})} + v_{\text{ne}}(\mathbf{r}) \\ &= \frac{\delta T_s[\rho]}{\delta \rho(\mathbf{r})} + v_H[\rho](\mathbf{r}) + v_{\text{xc}}[\rho](\mathbf{r}) + v_{\text{ne}}(\mathbf{r}) \\ &= \frac{\delta T_s[\rho]}{\delta \rho(\mathbf{r})} + v_{\text{eff}}^{\text{KS}}[\rho](\mathbf{r}) = \mu, \end{aligned} \quad (2)$$

where μ is the Lagrange multiplier to impose the correct

^{a)}Corresponding author. Electronic mail: yawang@chem.ubc.ca

normalization of $\rho(\mathbf{r})$ during the minimization and corresponds to the chemical potential after the total energy is minimized, and $v_{\text{H}}[\rho](\mathbf{r})$, $v_{\text{xc}}[\rho](\mathbf{r})$, and $v_{\text{eff}}^{\text{KS}}[\rho](\mathbf{r})$ are the Hartree, exchange-correlation, and total KS effective potentials, respectively. With the modern fast Fourier transform technique,¹⁶ OF-DFT can be implemented essentially as a linear-scaling method with computational cost of $\mathcal{O}(N \cdot \ln N)$.^{5,17-24} Studies on the dynamics of several thousand atoms near a metallic grain boundary,¹⁷ on the metal-insulator transition in a two-dimensional array of metal nanocrystal quantum dots,¹⁸ and in a multiscale model of nanoindentation¹⁹ demonstrate the power and efficiency of the OF-DFT method.

Although the research on OF-DFT has a much longer history than that on KS-DFT, OF-DFT has not yet become a mainstream QM method. The major obstacles lie in the lack of a transferable kinetic-energy density functional (KEDF) and accurate local pseudopotentials (LPSs) to calculate the kinetic energy and the nuclear-electron interaction energy.⁵ In the last decade, many linear-response based KEDFs have been developed, which can treat simple metallic systems almost as accurate as KS-DFT.^{20,21} Recently, first-principles LPSs derived from a bulk environment (BLPS) were generated for covalent materials²² and transition metals.²⁴ In KS-DFT, BLPSs accurately reproduce the results from high-quality nonlocal pseudopotentials (NLPS).²⁵ However, the use of such BLPSs in OF-DFT for covalent materials and transition metals produces results containing large unacceptable errors, which are mainly attributed to the defect of the approximate KEDFs.²²⁻²⁴ Thus, the present applications of OF-DFT are only confined to simple metallic systems.

To improve the present implementations of DFT and to further extend its application on large systems of thousands of atoms within different chemical bonding environment, we have devised a new OO-DFT method, which combines OF-DFT and KS-DFT via a density connection. In OO-DFT, one first solves Eq. (2) to obtain the density $\rho_{\text{OF}}(\mathbf{r})$ and the KS effective potential, $v_{\text{eff}}^{\text{KS}}[\rho_{\text{OF}}](\mathbf{r})$. Second, one solves the KS equations with the fixed $v_{\text{eff}}^{\text{KS}}[\rho_{\text{OF}}](\mathbf{r})$,

$$\left(-\frac{1}{2}\nabla^2 + v_{\text{eff}}^{\text{KS}}[\rho_{\text{OF}}](\mathbf{r})\right)\phi_i^{(1)}(\mathbf{r}) = \epsilon_i^{(1)}\phi_i^{(1)}(\mathbf{r}), \quad (3)$$

and obtains the new density $\rho_{\text{OO}}^{(1)}(\mathbf{r})$ after one non-self-consistent iteration,

$$\rho_{\text{OO}}^{(1)}(\mathbf{r}) = \sum_i f_i^{(1)}|\phi_i^{(1)}(\mathbf{r})|^2, \quad (4)$$

where $\epsilon_i^{(1)}$ and $f_i^{(1)}$ are the eigenvalue and occupation number of the i th KS orbital $\phi_i^{(1)}(\mathbf{r})$ of the first KS iteration, respectively. The above procedures constitute the essence of OO-DFT. With the above mentioned linear-scaling techniques for a fixed KS effective potential,⁴ the implementation of OO-DFT can be made essentially linear. Since $v_{\text{eff}}^{\text{KS}}(\mathbf{r})$ in Eq. (3) can be either local or nonlocal, the NLPS can thus be employed for $v_{\text{ne}}(\mathbf{r})$ in OO-DFT to eliminate the drawback of LPSs in OF-DFT.²²⁻²⁴ In OO-DFT, $\rho_{\text{OF}}(\mathbf{r})$ is the key link between OF-DFT and KS-DFT and its accuracy dictates the final results through $v_{\text{eff}}^{\text{KS}}[\rho_{\text{OF}}](\mathbf{r})$ in Eq. (3).

There are several ways to define the total energy in OO-DFT. Following Chelikowsky and Louie,²⁶ one can use the Hohenberg-Kohn-Sham (HKS) functional evaluated at $\rho_{\text{OO}}^{(1)}(\mathbf{r})$ as the total energy,

$$E^{\text{HKS}}[\rho_{\text{OF}}, \rho_{\text{OO}}^{(1)}] = \sum_i f_i^{(1)}\epsilon_i^{(1)} + E_{\text{H}}[\rho_{\text{OO}}^{(1)}] + E_{\text{xc}}[\rho_{\text{OO}}^{(1)}] - \langle \rho_{\text{OO}}^{(1)}(\mathbf{r})v_{\text{H}}[\rho_{\text{OF}}] \rangle - \langle \rho_{\text{OO}}^{(1)}(\mathbf{r})v_{\text{xc}}[\rho_{\text{OF}}] \rangle. \quad (5)$$

Alternatively, replacing $\rho_{\text{OO}}^{(1)}(\mathbf{r})$ by $\rho_{\text{OF}}(\mathbf{r})$ in Eq. (5), one obtains the famous Harris functional,¹¹

$$E^{\text{Harris}}[\rho_{\text{OF}}, \rho_{\text{OO}}^{(1)}] = \sum_i f_i^{(1)}\epsilon_i^{(1)} + E_{\text{xc}}[\rho_{\text{OF}}] - E_{\text{H}}[\rho_{\text{OF}}] - \langle \rho_{\text{OF}}(\mathbf{r})v_{\text{xc}}[\rho_{\text{OF}}] \rangle. \quad (6)$$

Normally, the HKS functional offers an upper bound to the self-consistent KS total energy, E^{KS} , while the Harris functional is stationary at the self-consistent KS electron density, $\rho_{\text{KS}}(\mathbf{r})$, and its value is usually lower than E^{KS} .¹¹ Therefore, we propose the following Zhou-Wang- λ (ZW λ) functional as a better approximation to E^{KS} via an error cancellation between E^{HKS} and E^{Harris} ,

$$E^{\text{ZW}\lambda}[\rho_{\text{OF}}, \rho_{\text{OO}}^{(1)}] = (1 - \lambda)E^{\text{HKS}}[\rho_{\text{OF}}, \rho_{\text{OO}}^{(1)}] + \lambda E^{\text{Harris}}[\rho_{\text{OF}}, \rho_{\text{OO}}^{(1)}], \quad (7)$$

where λ is an interpolation parameter. Based upon the work of Finnis,¹² the form of the ZW λ functional can be further rationalized on the ground that the second-order errors in E^{HKS} and E^{Harris} in Eq. (7) cancel if a linear combination of $\rho_{\text{OO}}^{(1)}(\mathbf{r})$ and $\rho_{\text{OF}}(\mathbf{r})$ provides a good approximation to $\rho_{\text{KS}}(\mathbf{r})$,

$$\rho_{\text{KS}}(\mathbf{r}) \approx (1 - \lambda)\rho_{\text{OO}}^{(1)}(\mathbf{r}) + \lambda\rho_{\text{OF}}(\mathbf{r}). \quad (8)$$

Understandably, the optimal value of λ for different systems depends on the quality of $\rho_{\text{OF}}(\mathbf{r})$ and $\rho_{\text{OO}}^{(1)}(\mathbf{r})$. Usually, a high-quality $\rho_{\text{OF}}(\mathbf{r})$ delivers an even better-quality $\rho_{\text{OO}}^{(1)}(\mathbf{r})$, which renders E^{HKS} more accurate than E^{Harris} , resulting in a small weight of E^{Harris} or a small value of λ in Eq. (7). However, the errors in $\rho_{\text{OF}}(\mathbf{r})$ and $\rho_{\text{OO}}^{(1)}(\mathbf{r})$ may be of similar magnitude for some systems, in which the weight of E^{Harris} should be increased to allow more error cancellation. With the optimal λ , $E^{\text{ZW}\lambda}$ should outperform both E^{HKS} and E^{Harris} in OO-DFT.

A similar idea of combining OF-DFT and KS-DFT also appeared in some implementations^{27,28} of the Strutinsky shell correction method,²⁹ in which the crude TF KEDF is usually employed in OF-DFT. The scheme of Yannouleas *et al.*²⁷ is equivalent to using the Harris functional in OO-DFT, while the scheme of Ullmo *et al.*²⁸ is similar to utilizing the HKS functional in OO-DFT. The OO-DFT method introduced here should be more general and better than these two schemes. Another approximation for the evaluation of the exact $\rho_{\text{KS}}(\mathbf{r})$ without running many self-consistent iterations was also suggested,²⁸ but we found it to be impractical in general.

Previously, our OF-DFT studies^{22,23} found that the state-of-the-art linear-response based KEDF, i.e., the Wang-Govind-Carter (WGC) KEDF with a density dependent

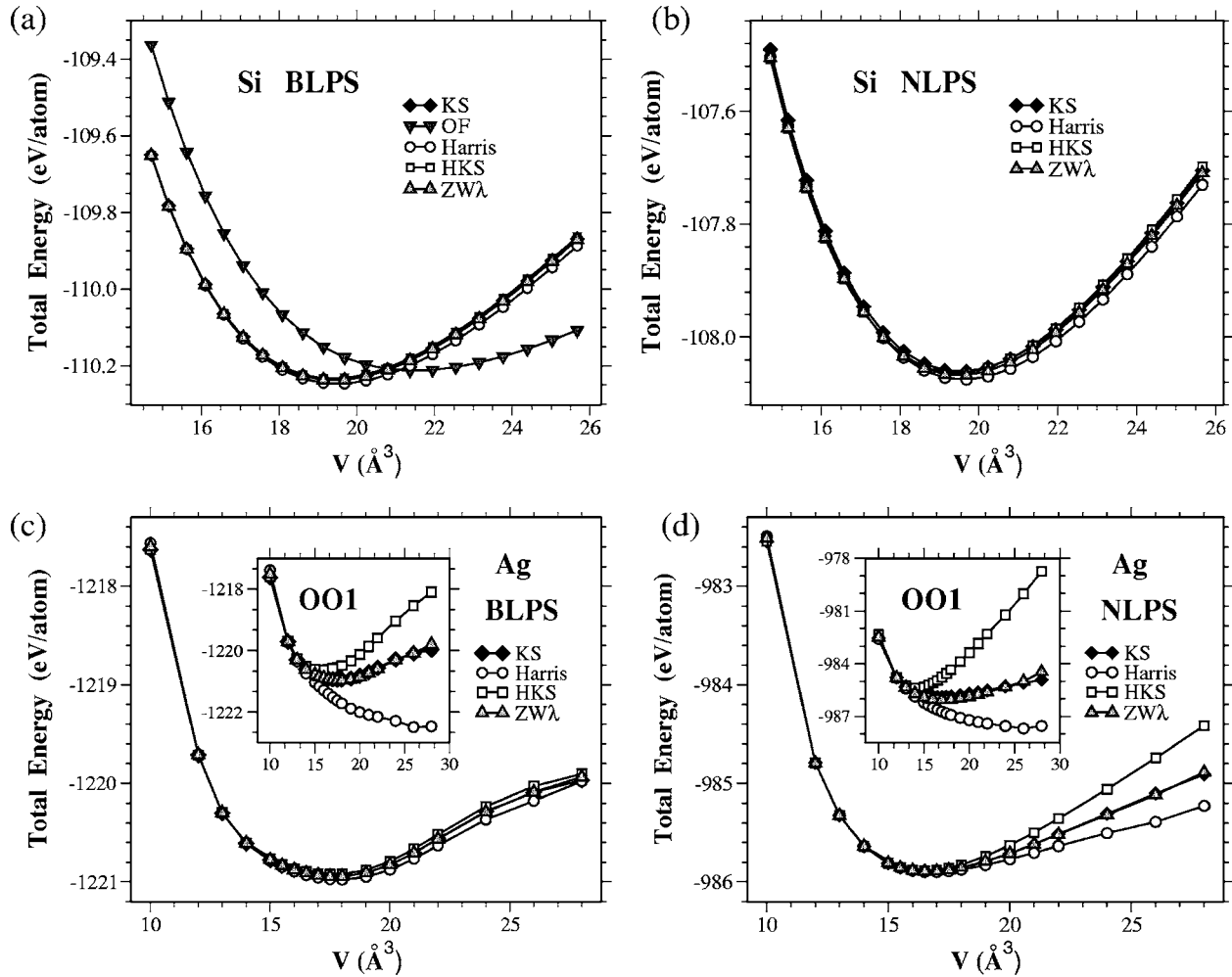


FIG. 1. LDA total energies (in eV/atom) vs cell volume V (in \AA^3) for the CD Si and the fcc Ag. In (a) and (c), the BLPSs were used. In (b) and (d), the NLPSs were used. In OO-DFT, the Harris (open circle), HKS (open square), and $ZW\lambda$ (opaque up triangle) functionals are used. In (a) and (b), OF-DFT (dark down triangle, only for the BLPS), OO1-DFT, and KS-DFT (solid diamond) results are compared with one another for the CD Si. In (c) and (d), KS-DFT results are compared with OO2-DFT results and the two insets show the comparison between KS-DFT and OO1-DFT results for the fcc Ag.

kernel,²¹ is inadequate to describe the covalent bonding in the cubic-diamond (CD) Si system. The bulk properties predicted by OF-DFT contain significant errors, although the resulting electron density is of much better quality. Below, we will test OO-DFT on the same system with a hope to reduce such errors from OF-DFT.

The local density approximation (LDA)³⁰ for the XCEDF was used for all DFT calculations in this work. The *ABINIT* code³¹ was modified to implement our OO-DFT method. In OO-DFT and KS-DFT, both the BLPS and the NLPS constructed from the standard Troullier-Martins scheme³² using the *FHI98PP* code³³ were used to compute the nuclear-electron interaction energy. A $6 \times 6 \times 6$ Monkhorst-Pack grid³⁴ with 40 irreducible \mathbf{k} -points was used in the Brillouin-zone sampling of an eight-atom cubic unit cell for the CD Si. In OO-DFT, the Harris, HKS, and $ZW\lambda$ functionals were used to evaluate the total energy. In OF-DFT calculations, the WGC KEDF with the optimized parameters^{21,23} and the BLPS²² were employed. The kinetic-energy cutoffs for the plane-wave basis set were chosen to be 760 eV for OO-DFT and KS-DFT calculations and 1.52 KeV for OF-DFT calculations to ensure all the quanti-

ties we computed are fully converged with respect to the basis set. A second-order damped dynamics method^{5,21} was employed to minimize the total energy with the convergence criterion set to 0.125 meV/atom.²³ Hereafter, we will use OO1 to denote the results from the first KS iteration.

The equations of state of the CD Si from OF-DFT, OO1-DFT, and KS-DFT are shown in Fig. 1. OF-DFT only produces qualitatively accurate equations of state, whereas the equations of state from KS-DFT are well reproduced in OO1-DFT using the Harris, HKS, and $ZW\lambda$ functionals with both of the BLPS and the NLPS [Figs. 1(a) and 1(b)]. However, the resemblance of the equations of state of the Harris and HKS functionals to those of KS-DFT is slightly degrading as the cell volume increases, which clearly reflects that the quality of $\rho_{\text{OF}}(\mathbf{r})$ is of the same trend. We also see that the errors in the Harris functional are larger than those in the HKS functional, which indicates that $\rho_{\text{OO}}^{(1)}(\mathbf{r})$ is prominently better than $\rho_{\text{OF}}(\mathbf{r})$ even at large cell volumes and anticipates a small optimal value for λ . With the BLPS, the $ZW\lambda$ energies almost exactly match those of KS-DFT using a small optimal λ value of 0.30. With the NLPS, the optimal λ value

increases only to 0.34, due to a slightly larger deviation of $\rho_{\text{OF}}(\mathbf{r})$ from $\rho_{\text{KS}}(\mathbf{r})$.

We then fitted the data of the equations of state to the Murnaghan's equation³⁵ and obtained the static bulk properties of the CD Si. The large errors in OF-DFT are nearly 11% for the equilibrium volume V_0 , 36% for the equilibrium bulk modulus B_0 , and 23.0 meV/atom for the equilibrium energy E_0 . These errors are sufficiently reduced in OO1-DFT with the use of the Harris, HKS, and ZW λ functionals. Among them, the ZW λ functional yields almost identical bulk properties to the KS-DFT predictions. With the use of the NLPS, the smallest errors are again in the ZW λ results: about 0.08% for V_0 , 0.2% for B_0 , and 1.0 meV/atom for E_0 . The improvement achieved by OO1-DFT for the CD Si is very encouraging indeed.

In our previous efforts to further extend OF-DFT to treat the face-centered-cubic (fcc) Ag,²⁴ it was found that the highly localized density distribution of the d electrons of Ag poses even harder challenges: the WGC KEDF^{5,21} failed to converge the total energy.²³ The von Weizsäcker- ξ -Thomas-Fermi (vW ξ TF) KEDF,³⁶ which incorporates a partial contribution ($\xi=0.4$) from the TF KEDF into the full von Weizsäcker (vW) KEDF³⁷ is more capable of dealing with systems with strongly localized electron distributions. For the fcc Ag, the use of the vW ξ TF KEDF and the BLPS in OF-DFT produces densities bearing a close resemblance to those from KS-DFT, but the equations of state still exhibit large unacceptable errors.²⁴ Such a transition metal system provides a stringent test on the robustness of our OO-DFT.

A kinetic-energy cutoff of 1.2 KeV was used in KS-DFT calculations. Both the BLPS²⁴ and the NLPS³² were employed to compute the nuclear-electron interaction energy. A $6 \times 6 \times 6$ Monkhorst-Pack grid with 40 irreducible \mathbf{k} -points was used for the Brillouin-zone sampling of a four-atom cubic unit cell for the fcc Ag. Fermi-surface smearing of width 54 meV was utilized to converge the KS orbitals at the Fermi level. In OF-DFT, the real space grids were set to be the same as those used in KS-DFT. Due to the nature of the extremely repulsive BLPS and the highly localized density distributions, almost all the grid points in the corresponding reciprocal space grids were used to compute the nuclear-electron interaction energy and the vW kinetic energy. Thus, the maximum energy of the plane waves reaches *ca.* 10 KeV.²⁴ As shown later, the first KS iteration gets rid of most of the errors in OF-DFT. However, the remaining errors are still significant. This motivates us to introduce the second KS iteration in OO-DFT. To avoid the well-known "density sloshing" problem,¹⁰ the input density for the second KS iteration $\rho_{\text{in}}^{(2)}(\mathbf{r})$ was chosen to be the average of $\rho_{\text{OF}}(\mathbf{r})$ and $\rho_{\text{OO}}^{(1)}(\mathbf{r})$. Consequently, $\rho_{\text{OF}}(\mathbf{r})$ and $\rho_{\text{OO}}^{(1)}(\mathbf{r})$ in Eqs. (5)–(7) are replaced by $\rho_{\text{in}}^{(2)}(\mathbf{r})$ and the output density of the second KS iteration, $\rho_{\text{OO}}^{(2)}(\mathbf{r})$, respectively. Hereafter, we will use OO2 to denote the results from the second KS iteration.

The equations of state of the fcc Ag from OO1-DFT and KS-DFT are displayed in the insets of Fig. 1 for both of the BLPS and the NLPS. In both cases, the equations of state produced from the Harris and HKS functionals contain large errors, which increase significantly with the increase of the

cell volume, although they closely match the equations of state from KS-DFT at small volumes. As shown by the insets of Fig. 1(c), the errors in the Harris functional is larger than those in the HKS functional when the BLPS is used, resulting an optimal λ value of 0.39. On the other hand, with the NLPS, E^{Harris} is closer to E^{KS} than E^{HKS} is, especially at large volumes. This clearly implies that $\rho_{\text{OO}}^{(1)}(\mathbf{r})$ is severely overcorrected in the first KS iteration. Thus, it is not surprising to find the optimal λ value increases to 0.65. The ending result is very exciting: the ZW λ functional yields much more accurate equations of state than the HKS and Harris functionals do.

The second KS iteration brings remarkable improvements to the equations of state, as illustrated in Fig. 1. With the BLPS [Fig. 1(c)], both the Harris and HKS functionals generate equations of state that are only slightly off at large volumes. The ZW λ functional almost exactly reproduces the equations of state of KS-DFT when λ equals 0.41. With the NLPS [Fig. 1(d)], the equations of state from the Harris and HKS functionals still exhibit significant errors at large cell volumes. This indicates that the errors in $\rho_{\text{OF}}(\mathbf{r})$ at large volumes are too large to be completely eliminated even by the second KS iteration. However, these errors miraculously diminish in the equations of state produced by the ZW λ functional when λ equals 0.58. Note that the optimal λ values of the BLPS and the NLPS in OO2-DFT are very close to those in OO1-DFT.

The static bulk properties of the fcc Ag were again computed. With the use of the BLPS in OO1-DFT, the ZW λ functional produces reasonably accurate results, deviating from KS-DFT results only 2.7% for V_0 , 2.6% for B_0 , and 0.020 eV/atom for E_0 . When the NLPS is used, these errors increase somewhat, but still acceptable: 1.2% for V_0 , 19.5% for B_0 , and 0.15 eV/atom for E_0 . In OO2-DFT, these errors are effectively suppressed by the ZW λ functional. With the BLPS, the deviations from KS-DFT predictions are less than 0.09% for V_0 , 1.6% for B_0 , and virtually zero for E_0 . With the NLPS, they are 0.02% for V_0 , 1.5% for B_0 , and 4.0 meV/atom for E_0 . This confirms that our OO-DFT method is very versatile and robust: OO-DFT can even handle systems involving large density fluctuations and strong density localizations, such as transition metals.

Given those well-established linear-scaling KS-DFT and OF-DFT algorithms,^{4,5,7,8,17–24} OO-DFT can certainly be implemented as a highly powerful linear-scaling QM method capable of treating large systems of thousands of atoms accurately. The central technical issue of OO-DFT is to obtain an optimal λ value, which depends on the chemical environment of the system under study and is not very sensitive to the size of the system. For example, for the CD Si, the optimal λ value remains the same whether we use an eight-atom unit cell or a 64-atom supercell or even bigger cells. Thus, for the large-scale application of OO-DFT, a simple, straightforward way to determine the optimal λ value is to find the optimal λ value for a small subsystem, whose chemical environment closely mimics that of the entire system, and use the same λ value in subsequent OO-DFT calculations for the entire system. Currently, we are developing a new scheme to determine the optimal λ value *a priori*.

In conclusion, our OO-DFT remedies the drawbacks of OF-DFT: the lack of a transferable KEDF and accurate LPSS, at the cost of only introducing a single or double non-self-consistent KS iterations, which in turn basically eliminates the necessity for a full self-consistent KS cycle. Two irrevocable factors have contributed to the success of our OO-DFT method: (i) the high-quality $\rho_{\text{OF}}(\mathbf{r})$ as the input density from OF-DFT calculation with the state-of-the-art KEDFs and the BLPSs^{5,17-24} and (ii) the built-in systematic error cancellation in the ZW λ functional between the Harris and HKS functionals. Due to the linear-scaling nature of OO-DFT, we may treat large systems of thousands of atoms and venture into regions beyond the limits of other first-principles QM methods currently available in the literature.

Financial support for this project was provided by a grant from the Natural Sciences and Engineering Research Council of Canada. The authors are grateful for discussions with Professor Emily A. Carter.

¹R. G. Parr and W. Yang, *Density-Functional Theory of Atoms and Molecules* (Clarendon, New York, 1989); R. M. Dreizler and E. K. U. Gross, *Density Functional Theory: An Approach to the Quantum Many-Body Problem* (Springer-Verlag, Berlin, 1990).

²P. Hohenberg and W. Kohn, Phys. Rev. **136**, B864 (1964).

³W. Kohn and L. J. Sham, Phys. Rev. **140**, A1133 (1965).

⁴S. Goedecker, Rev. Mod. Phys. **71**, 1085 (1999); W. Kohn, Phys. Rev. Lett. **76**, 3168 (1996).

⁵Y. A. Wang and E. A. Carter, in *Theoretical Methods in Condensed Phase Chemistry*, edited by S. D. Schwartz (Kluwer, Dordrecht, 2000), p. 117.

⁶N. W. Ashcroft and N. D. Mermin, *Solid State Physics* (Saunders, Orlando, 1976).

⁷F. Shimojo, R. K. Kalia, A. Nakano, and P. Vashishta, Comput. Phys. Commun. **140**, 303 (2001).

⁸J. M. Soler, E. Artacho, J. D. Gale, A. García, J. Junquera, P. Ordejón, and D. Sánchez-Portal, J. Phys.: Condens. Matter **14**, 2745 (2002); C. Skylaris, P. D. Haynes, A. A. Mostofi, and M. C. Payne, J. Chem. Phys. **122**, 084119 (2005).

⁹G. Kresse and J. Furthmüller, Phys. Rev. B **54**, 11169 (1996).

¹⁰J. F. Annett, Comput. Mater. Sci. **4**, 23 (1995).

¹¹J. Harris, Phys. Rev. B **31**, 1770 (1985); H. M. Polatoglou and M. Methfessel, *ibid.* **37**, 10403 (1988); A. J. Read and R. J. Needs, J. Phys.: Condens. Matter **1**, 7565 (1989); E. Zaremba, *ibid.* **2**, 2479 (1990); I. J. Robertson and B. Farid, Phys. Rev. Lett. **66**, 3265 (1991).

¹²M. W. Finnis, J. Phys.: Condens. Matter **2**, 331 (1990).

¹³D. M. Benoit, D. Sebastiani, and M. Parrinello, Phys. Rev. Lett. **87**, 226401 (2001).

¹⁴W. Zhu and S. B. Trickey, Int. J. Quantum Chem. **100**, 245 (2004).

¹⁵L. H. Thomas, Proc. Cambridge Philos. Soc. **23**, 542 (1927); E. Fermi, Rend. Accad. Naz. Lincei **6**, 602 (1927); E. Fermi, Z. Phys. **48**, 73 (1928).

¹⁶W. H. Press, B. P. Flannery, S. A. Teukolsky, and W. T. Vetterling, *Numerical Recipes in Fortran* (Cambridge University Press, Cambridge, 1992).

¹⁷S. C. Watson and P. A. Madden, PhysChemComm **1**, 1 (1998).

¹⁸S. C. Watson and E. A. Carter, Comput. Phys. Commun. **128**, 67 (2000).

¹⁹M. Fago, R. H. Hayes, E. A. Carter, and M. Ortiz, Phys. Rev. B **70**, 100102 (2004).

²⁰L.-W. Wang and M. P. Teter, Phys. Rev. B **45**, 13196 (1992); E. Smargiassi and P. A. Madden, *ibid.* **49**, 5220 (1994); M. Foley and P. A. Madden, *ibid.* **53**, 10589 (1996); Y. A. Wang, N. Govind, and E. A. Carter, *ibid.* **58**, 13465 (1998); Erratum: *ibid.* **64**, 129901 (2001); F. Perrot, J. Phys.: Condens. Matter **6**, 431 (1994).

²¹Y. A. Wang, N. Govind, and E. A. Carter, Phys. Rev. B **60**, 16350 (1999); Erratum: *ibid.* **64**, 089903 (2001).

²²B. Zhou, Y. A. Wang, and E. A. Carter, Phys. Rev. B **69**, 125109 (2004).

²³B. Zhou, V. L. Lignères, and E. A. Carter, J. Chem. Phys. **122**, 044103 (2005).

²⁴B. Zhou and E. A. Carter, J. Chem. Phys. **122**, 184108 (2005).

²⁵W. E. Pickett, Comput. Phys. Rep. **9**, 115 (1989).

²⁶J. R. Chelikowsky and S. G. Louie, Phys. Rev. B **29**, 3470 (1984).

²⁷C. Yannouleas, E. N. Bogachek, and U. Landman, Phys. Rev. B **57**, 4872 (1998).

²⁸D. Ullmo, T. Nagano, S. Tomsovic, and H. U. Baranger, Phys. Rev. B **63**, 125339 (2001).

²⁹V. M. Strutinsky, Nucl. Phys. A **122**, 1 (1968); M. Brack, J. Damgaard, A. S. Jensen, H. C. Pauli, V. M. Strutinsky, and C. Y. Wong, Rev. Mod. Phys. **44**, 320 (1972); D. Ullmo, H. Jiang, W. Yang, and H. U. Baranger, Phys. Rev. B **70**, 205309 (2004).

³⁰J. P. Perdew and A. Zunger, Phys. Rev. B **23**, 5048 (1981).

³¹X. Gonze, J.-M. Beuken, R. Caracas *et al.*, Comput. Mater. Sci. **25**, 478 (2002).

³²N. Troullier and J. L. Martins, Phys. Rev. B **43**, 1993 (1991).

³³M. Fuchs and M. Scheffler, Comput. Phys. Commun. **119**, 67 (1999).

³⁴H. J. Monkhorst and J. D. Pack, Phys. Rev. B **13**, 5188 (1976).

³⁵F. D. Murnaghan, Proc. Natl. Acad. Sci. U.S.A. **30**, 244 (1944).

³⁶J. Goodisman, Phys. Rev. A **1**, 1574 (1970); P. K. Acharya, L. J. Bartolotti, S. B. Sears, and R. G. Parr, Proc. Natl. Acad. Sci. U.S.A. **77**, 6978 (1980); J. L. Gázquez and J. Robles, J. Chem. Phys. **76**, 1467 (1982).

³⁷C. F. von Weizsäcker, Z. Phys. **96**, 431 (1935).

³⁸This is true even for metallic systems, as convincingly argued by the "nearsightedness" principle of Kohn (Ref. 4).